Ultra-Low Power Silicon Neuron Circuit for Extreme-Edge Neuromorphic Intelligence

Arianna Rubino*, Melika Payvand*, and Giacomo Indiveri*
*Institute of Neuroinformatics, University of Zurich and ETH Zurich

***Abstract*—Recent years have seen an increasing interest in the development of artificial intelligence circuits and systems for cloud-less edge computing applications. In an effort to reduce power consumption even further, we propose beyond von-Neumann in-memory computing architectures that can process the signals at the sensor side using ultra-low power mixed-signal analog/digital circuits which have properly matched dynamics and time-constants. In this paper, we propose one of the main computing elements of such architectures, namely the silicon neuron, designed using analog circuits in an advanced FDSOI 22 nm node. Here we optimize the design of an Adaptive Exponential Integrate and Fire (AdExp IF) neuron model for producing neural dynamics with biologically plausible time constants. We explore the options of the 22 nm FDSOI technology to address the analog design issues that arise from advanced scaling (such as leakage) and minimize power consumption by using a novel current comparator circuit with current-driven positive feedback. We present circuit simulation results which reproduce biologically plausible responses and compare the circuit energy per spike with state-of-the-art architectures. The proposed neuron design consumes one order of magnitude less power compared to the state-of-the-art and two orders of magnitude less compared to a pure digital implementation.**

***Index Terms*—Neuromorphic edge computing, Silicon neurons, FDSOI, Ultra-low power processing**

I. Introduction

As the amount of data generated by the connected devices are ever more increasing, the power consumption for processing them is becoming more and more relevant. Local edge computing is gaining considerable attention because it promises to bring significant power savings by avoiding data transfer to remote (cloud) computing systems. In an effort to reduce power consumption even further, we propose to endow edge-computing sensory devices with ultra-low power processing circuits that can continuously monitor the data-streams directly on the sensing node, extract relevant information, and activate more powerful (and power hungry) computing or communication systems only when necessary. Recurrent spiking neural networks (SNNs) have been shown to be an ideal model for implementing such type of processing, provided their time constants are well matched to those of the signals of interest [1]. Mixed-signal event-driven neuromorphic circuits are natural candidates for implementing such SNN architectures and integrating them directly into IoT sensor nodes [2]. These SoC embedded sensory-processing systems can then run SNN artificial intelligence learning and inference algorithms in real-time on the sensed signals and dramatically reduce the bandwidth of their output signals. We denote this approach as "extreme-edge neuromorphic intelligence". Such hardware is also suited for emerging memory technologies (e.g. memristors) and for the implementation of machine learning algorithms based on neural networks [3], [4]. However, mixed analog-digital design with deep sub-micron technology is challenging as a result of the increased leakage current that in advanced complementary metal-oxide-semiconductor processes becomes a significant portion of transistor's ON current, leading to an increase in power consumption. Finally, as the technology node scales down and the transistor's channel length decreases, its parameter variations (e.g. the threshold voltage) increase, and device mismatch increases even further.

In this paper, we present a sub-threshold neuron circuit that has been designed to implement large-scale multi-neuron multi-core neuromorphic computing architectures using a 22 nm Fully-Depleted Silicon on Insulator (FDSOI) process. We show how it is possible to implement bio-physically complex neural dynamics using ultra-low power compact analog circuits in advanced scaled processes, by analyzing the features of the 22 nm FDSOI technology and addressing the analog design issues that arise from the advanced scaling. To highlight the sub-parts of the 22 nm FDSOI silicon neuron circuits that are more sensitive to mismatch, we present Monte Carlo analysis results. Furthermore, we show how the use of an optimized current comparator with current-driven positive feedback significantly reduces power consumption.

II. Materials and Methods

In 180 nm or even larger processes, transistors in sub-threshold regime usually operate with currents in the range of a few pico-Amperes to tens of nano-Amperes. In more advanced processes minimum-size transistors have considerably larger leakage currents. Therefore, to maintain the desired range of low currents, we performed circuit simulations of single transistors and determined their proper geometrical size. The devices available in the 22 nm FDSOI technology differ on the threshold voltage (V_{th}) value and hence on the I_{off} as the two parameters are inversely proportional. Since our constraints are slow dynamics and low leakage, we considered the devices with high V_{th}, namely Ultra Low Leakage High Threshold Voltage Transistors (UHVT). As is illustrated in Fig. 1, by sweeping the width (80 nm - 600 nm) of both UHVT n-type and p-type with maximum length (36 nm), we determined the desired values of I_{off}. Based on these results, we designed an

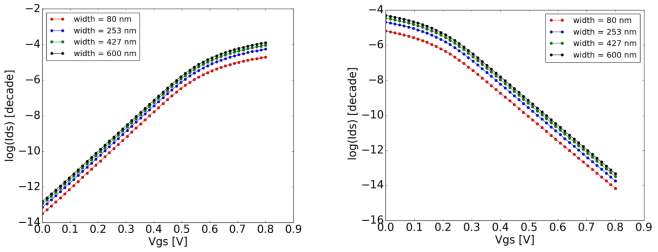

(a) (b)

Fig. 1. 22 nm FDSOI transistor geometrical analysis: (a) UHVT nfet I_{ds} vs V_{gs} sweeps for different widths and maximum length, (b) left analogous sweeps for a UHVT pfet device.

Adaptive Exponential Integrate-and-Fire (AdExp IF) neuron circuit using UHVT MOSFETs provided by the 22 nm FDSOI technology. The circuit (Fig. 2) comprises an input Differential Pair Integrator (DPI) [5], [6] filter (P1 - N4), a current-based positive feedback module (P7 - N10), a current comparator (CC) block (P15 - N17), a spike reset circuit with refractory period functionality (P13 - N21), a spike generation inverter (P12 - N22) and a spike-frequency adaptation mechanism implemented with an additional DPI filter (see Fig.2(b)).

The input DPI models the neurons leak conductance, producing exponential sub-threshold dynamics in response to constant input currents. The integrating capacitance C_{mem} (1 pF) represents the neurons membrane capacitance. The CC compares I_{mem} with I_{thr}, set by an external bias, which sets the neuron's spiking threshold. The positive feedback circuit models both sodium channel activation and inactivation dynamics, while the reset and refractory period circuit represents the potassium conductance functionality. The spike-frequency adaptation DPI models the neurons calcium conductance, and produces an after-hyperpolarization current (I_{en_adp}) proportional to the neurons mean firing rate. The neuron and the spike-frequency adaptation circuits are connected by a pulse extender which extends the spike duration.

To limit the Early effect, we used pseudo-cascode split-transistor sub-threshold technique, as done in [7]. This technique allows to generate bias currents on the order of pico-Amperes, necessary to have large time constants, while keeping the size of the capacitors to a minimum. For example, the diode-connected transistors N1-N2 in Fig. 2(a) and 2(b) are added to reduce the V_{ds} of the transistors P3 and P4 respectively.

We used the same split-transistor sub-threshold technique for the bias current-mirrors, in order to compensate for mismatch, and to enhance current mirror operation to have precise control of small currents. Similarly, all the circuit parameters that require currents on the order of a few pico-Amperes have been implemented using transistors in series.

All capacitors are implemented using the Alternate Polarity Metal On Metal (APMOM) option. The value of the capacitance and the size are shown in Table I.

TABLE I
CAPACITANCE VALUES AND SIZES USED IN THE DESIGN

	C_{mem}	C_{ahp}	C_{ref}	C_{pex}
Value	1 pF	2 pF	700 fF	600 fF
Width	20 μm	28 μm	16 μm	15 μm
Length	20 μm	30 μm	19 μm	17 μm

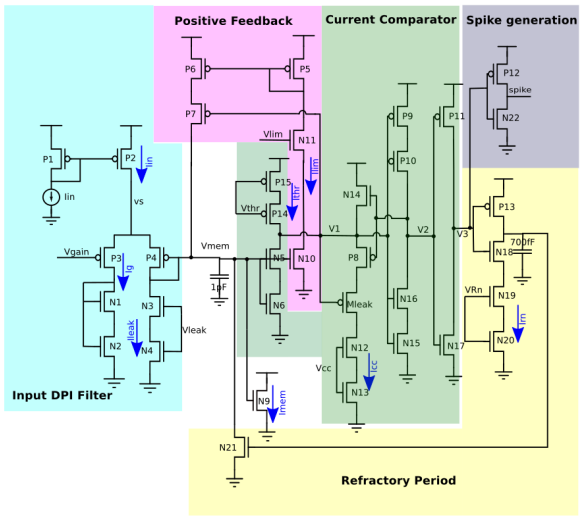

(a)

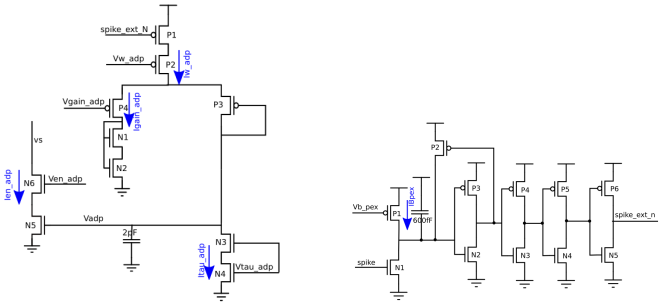

(b) (c)

Fig. 2. 22 nm FDSOI AdExp IF neuron schematic: (a) Neuron circuit schematic with sub-parts: DPI input filter (light blue), Positive feedback (magenta), Current comparator (green), Refractory period circuitry (yellow) and spike-generation inverter (grey). (b) Spike-frequency adaptation circuit schematic (AHP). (c) Pulse extender schematic (PEX).

III. Results and Discussion

A. Circuit simulations

We optimized the design of the AdExp IF neuron for producing biologically plausible neural dynamics, with time constants matched to those of natural signals, such as speech or bio-signals.

Simulation results demonstrating examples of biologically plausible behaviors are shown in Fig. 3. Figure 3(a) shows the neuron spiking frequency versus input current (F-I curve), for different settings of the I_{gain} bias. As expected, increases in I_{gain} result in the increase of the neuron's firing rate.

Figure 3(b) shows the neuron's F-I curve for different I_{ref} bias settings. As the I_{ref} increases, the refractory period is shorter and hence the neuron's maximum spiking frequency increases. Figure 4 demonstrates the spike-frequency adaptation behavior, obtained by appropriately tuning the relevant parameters in the AHP block of Fig. 2 and stimulating the neuron with a constant injection current.

The time constant of the spike-frequency adaptation circuit

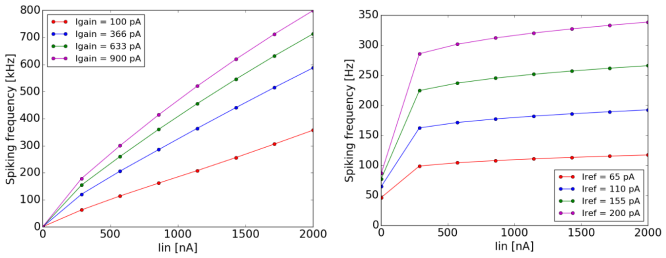

(a) (b)

Fig. 3. Spiking frequency vs Input current sweeping two neuron biases: I_{gain} (a) and I_{ref} (b) to evaluate whether the neuron is able to simulate a biological response

(63 ms) is twice the time constant of the neuron circuit (31 ms) since the capacitance C_{ahp} (2 pF) is twice C_{mem} (1 pF) using both I_{leak} and I_{tau_adp} equal to 1 pA.

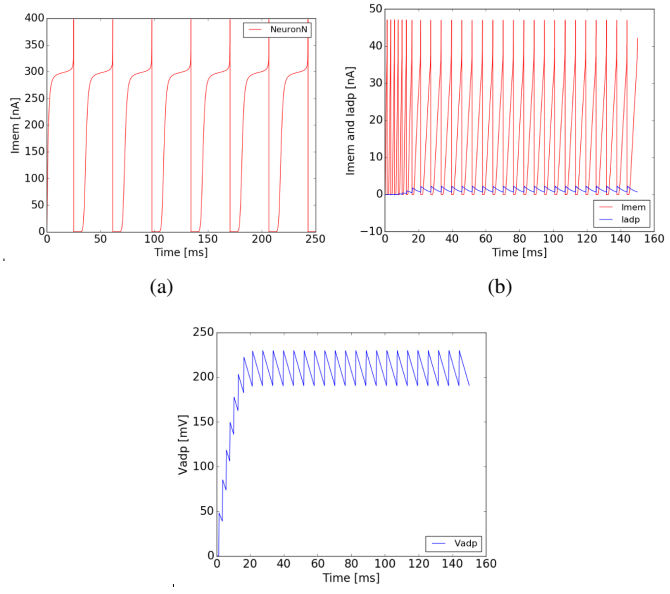

(a) (b)

(c)

Fig. 4. Biologically plausible behaviour: (a) Membrane current I_{mem} shape over time. (b) and (c) Spike-frequency adaptation: (b) I_{mem} and I_{adp} trace over time, (c) V_{adp} trace over time

B. Energy per spike

Once proven that the design is able to reproduce a biologically plausible behaviour, we evaluated whether it can implement massively parallel large-scale neuromorphic processors. We compare the energy per spike of the neuron proposed in this work with previously proposed state-of-the-art neuromorphic processors in Table II.

The neuron designed in this work consumes one order of magnitude less compared to the most recent silicon neuron circuit design, the Sigma-Delta neuron proposed in [10].

TABLE II
ENERGY PER SPIKE COMPARISON WITH PREVIOUS WORKS

Work	[8]	[9]	[10]	[11]	**This work**
Techn.	180 nm	28 nm	180 nm	28 nm	22 nm
Type	Mixed	Mixed	Mixed	Digital	Mixed
V_{dd}	1.8 V	0.7 V-1 V	1.8 V	0.775 V	0.8 V
En./spike	883 pJ	2.3 nJ-30 nJ	10 pJ	800 pJ	990 fJ

C. Monte Carlo Analysis

We ran Monte Carlo simulations to evaluate the sensitivity of the circuit to mismatch. We performed this analysis with 500 runs for this neuron circuit, with DC current injected through P2 in Fig. 2, and with bias currents set to obtain a firing rate of approximately 65 Hz while switching off the spike-frequency adaptation circuit.

The Monte Carlo simulation produces a bi-modal distribution

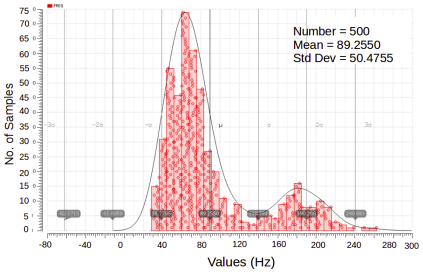

Fig. 5. Monte Carlo simulation distribution of the neuron circuit

(see Fig. 5). The first mode gives a Gaussian distribution around the expected frequency value, 65 Hz. The second mode, shows that the neuron can fire at higher frequencies, around 180 Hz - 200 Hz. One possible reason for this could be that some parts of the circuit are faster than the refractory period part and make the neuron fire at higher frequencies exceeding the maximum value. In fact, the refractory period circuitry limits the neuron to fire with a maximum frequency of 100 Hz. If another part of the circuit is stronger than the refractory period, the node V_{mem} does not reset completely staying at a higher voltage value. In this way, the neuron reaches the spiking threshold faster leading to higher spiking frequencies. We performed further Monte Carlo analysis to understand which specific transistors give this bi-modal distribution. Firstly, taking into account the mismatch sensitivity of the single neuron circuit. Secondly, considering also the sensitivity of the bias current mirrors. The result is reported in Fig. 6: In red the transistors that show sensitivity to mismatch by simulating the circuit without including the bias current mirrors and in orange the additional transistors that show sensitivity

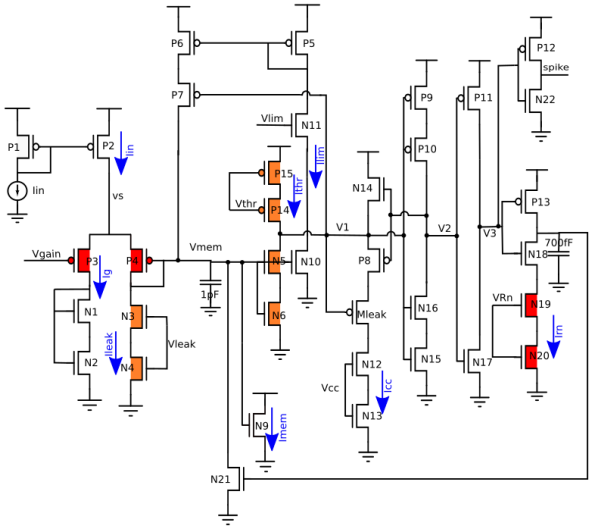

(a)

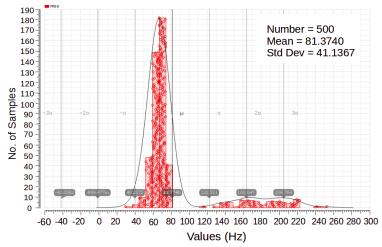

(b)

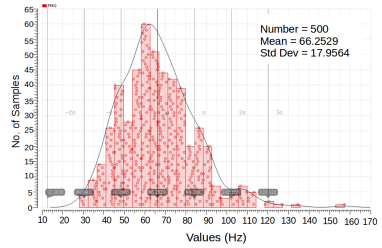

(c)

Fig. 6. Monte Carlo analysis: (a) Neuron circuit with transistors more sensitive to mismatch highlighted: In red/orange are the transistors with more sensitivity to mismatch from the Monte Carlo analysis of the circuit without/with considering the bias current mirrors. (b) Sensitivity distribution of the input DPI filter. (c) Sensitivity distribution of the refractory period part

when including the current mirrors. Therefore, to optimize the circuit, transistors in series and in parallel must be added in order to decrease the variability caused by mismatch. This modification can be done just for the more sensitive sub-parts of the circuit highlighted with this analysis (Fig. 6).

IV. Conclusion

We determined process and circuit parameters in order to implement efficient (low power and low mismatch) analog neuron circuits using an advanced scaled 22 nm FDSOI process. The neuron circuit presented has an energy per spike of the order of 10^{-13} - 10^{-12}, which is considerably lower compared to an analogous neuron design implemented in a 180 nm CMOS process [8]. Furthermore analysis has shown how the proposed 22 nm implementation of the analog/digital IF AdExp neuron consumes two orders of magnitude less per spike than fully digital implementations.

We studied with Monte Carlo analysis the mismatch sensitivity of the neuron circuit and highlighted the parts of the circuit that are most critical to be optimized for variations. In particular, we showed how the more sensitive sub-parts of the silicon neuron circuit are the input DPI filter, the first part of the CC, and the refractory period part. To minimize the effect of device mismatch we set the length and width of the most sensitive transistors to larger values.

Acknowledgment

This work is supported by the European Union's Horizon 2020 ERC project NeuroAgents (Grant No. 724295), and Toshiba Corporation. This project has also received funding from the ECSEL Joint Undertaking (JU) under grant agreement No 826655. The JU receives support from the European Unions Horizon 2020 research and innovation programme and Belgium, France, Germany, Netherlands, Switzerland

References

[1] G. Indiveri and Y. Sandamirskaya, "The importance of space and time in neuromorphic cognitive agents," *arXiv preprint arXiv:1902.09791*, 2019.

[2] S. Moradi, S. A. Bhave, and R. Manohar, "Energy-efficient hybrid CMOS-NEMS LIF neuron circuit in 28 nm CMOS process," in *2017 IEEE Symposium Series on Computational Intelligence (SSCI)*, Nov 2017, pp. 1–5.

[3] M. Payvand, M. Nair, L. Müller, and G. Indiveri, "A neuromorphic systems approach to in-memory computing with non-ideal memristive devices: From mitigation to exploitation," *Faraday Discussions*, pp. 1–13, 2018. [Online]. Available: http://dx.doi.org/10.1039/C8FD00114F

[4] G. Indiveri, F. Corradi, and N. Qiao, "Neuromorphic architectures for spiking deep neural networks," in *Electron Devices Meeting (IEDM), 2015 IEEE International*. IEEE, Dec. 2015, pp. 4.2.1–4.2.14.

[5] C. Bartolozzi and G. Indiveri, "Synaptic dynamics in analog VLSI," *Neural Computation*, vol. 19, no. 10, pp. 2581–2603, Oct 2007.

[6] C. Bartolozzi, S. Mitra, and G. Indiveri, "An ultra low power current–mode filter for neuromorphic systems and biomedical signal processing," in *Biomedical Circuits and Systems Conference, (BioCAS), 2006*. IEEE, 2006, pp. 130–133.

[7] N. Qiao and G. Indiveri, "Analog circuits for mixed-signal neuromorphic computing architectures in 28 nm fd-soi technology," in *Proceedings of the 2017 IEEE SOI-3D-Subthreshold Microelectronics Technology Unified Conference (S3S)*. IEEE, 2017.

[8] S. Moradi, N. Qiao, F. Stefanini, and G. Indiveri, "A scalable multicore architecture with heterogeneous memory structures for dynamic neuromorphic asynchronous processors (DYNAPs)," *Biomedical Circuits and Systems, IEEE Transactions on*, vol. 12, no. 1, pp. 106–122, Feb. 2018.

[9] C. Mayr, J. Partzsch, M. Noack, S. Hänzsche, S. Scholze, S. Höppner, G. Ellguth, and R. S. 2, "A biological-realtime neuromorphic system in 28 nm cmos using low-leakage switched capacitor circuits," *IEEE Transactions on Biomedical circuits and systems*, vol. 10, no. 1, pp. 243 – 254, 2016.

[10] M. V. Nair and G. Indiveri, "An ultra-low power sigma-delta neuron circuit," in *2019 IEEE International Symposium on Circuits and Systems (ISCAS)*, May 2019, pp. 1–5.

[11] P. A. Merolla, J. V. Arthur, R. Alvarez-Icaza, A. S. Cassidy, J. Sawada, F. Akopyan, B. L. Jackson, N. Imam, C. Guo, Y. Nakamura, B. Brezzo, I. Vo, S. K. Esser, R. Appuswamy, B. Taba, A. Amir, M. D. Flickner, W. P. Risk, R. Manohar, and D. S. Modha, "A million spiking-neuron integrated circuit with a scalable communication network and interface," *Science*, vol. 345, no. 6197, pp. 668–673, Aug 2014. [Online]. Available: http://www.sciencemag.org/content/345/6197/668